

Original Articles

Inhibition of Cell Growth and Induction of Apoptosis by *Euonymus Alatus* (Thunb.) Sieb in Human Leiomyomal Smooth Muscle Cells

Yi-Geun Kim¹⁾, Ji-Young Han¹⁾, Young-Soo Park¹⁾, Dong-Il Kim¹⁾,
Tae-Kyun Lee²⁾

Department of Gynecology, College of Oriental Medicine, Dongguk University¹⁾.
Dr. Lee's Traditional Korean Medical Clinic²⁾

Objective : *Euonymus alatus* (Thunb.) Sieb (EA) is a traditional Korean herbal medicine, commonly used to treat tumors in Korea and China for centuries. Several earlier studies have indicated that EA exhibits anti-tumor properties, but its mechanism remains to be elucidated. In this study, we evaluated the molecular mechanism of EA in a human uterine leiomyomal smooth muscle cell (ULSMC) line.

Methods : This study was evaluated by: (a), morphological changes by using acridine orange/ethidium bromide staining; (b), DNA fragmentation by TdT-mediated dUTP nick end labeling (TUNEL); and (c), sub-G1 cell analysis.

Results : This study observed that EA treatment caused apoptotic cell death and depletion of intracellular glutathione (GSH) and that reduction of mitochondrial membrane potential was found to be involved in the initiation of apoptosis by EA.

Conclusion : This results show that EA exerted clear cytotoxic effects and strongly inhibited the proliferation of ULSMC.

Key Words: *Euonymus alatus* (Thunb.) Sieb (EA); uterine leiomyomal smooth muscle cells (ULSMC); myometrial smooth muscle cells (MSMC).

Introduction

Euonymus alatus (Thunb.) Sieb (EA) is a herbal plant that has been widely used in traditional Korean and Chinese medicine for the treatment of tumors.

Euonymus alatus (Thunb.) Sieb, known as 'gui-jun woo' in Korea, was used in folk medicine to regulate qi (bodily energy) and blood circulation, relieve pain, eliminate stagnant blood, and treat dysmenorrhea in eastern asian countries. It can increase tolerance to oxygen deprivation, and has a significant, albeit temporary, hypotensive effect. It acts as a depressant on the CNS and can lengthen barbiturate-induced sleeping times. Its effects on metabolism include a reduction of blood sugar levels via stimulation of the beta cells of pancreatic islets. Additionally, quercetin has been found to be a good expectorant⁵⁾.

The antimetastatic and cytotoxic activity of the crude

Received 28 October 2004; Received in Revised from 7 November 2004; Accepted 12 November 2004

Correspondent to : Dong-Il Kim

Gangnam Oriental Medical Hospital, Dongguk University. 37-21 Nonhyun-Dong, Gangnam-Gu, Seoul 135-010, Korea. Tel : 82-2-3416-9737, Fax : 82-2-3416-9770, E-mail : obgykdi@netian.com

extract or the isolated compounds, however, have not yet been demonstrated. The stems of *Euonymus alatus* (Thunb.) Sieb, commonly known as winged euonymus, have been used in traditional medicine for tumor treatment. Previous phytochemical and biological studies on winged euonymus have resulted in the isolation of cardenolides¹⁾. Substances isolated from *Euonymus alatus* (Thunb.) Sieb have been documented to exhibit antioxidant capabilities, and recent studies also indicated that EA has anti-tumor potential²⁾. It was reported that the crude extract of EA markedly prolonged the survival period of cervical carcinoma-bearing mice, and methanol extract from this plant³⁾. Methanol and buthanol extracts were also found to have anti-tumor activity in mice⁴⁾. Moreover, there are some reports on the action of EA extract on transformed cells in vitro^{5,6)}. It was recently found that the methanolic extract of EA exhibited a significant anti-proliferation effect against cultured human cancer cell lines⁴⁾. Our recent findings also suggest that EA is a potent antioxidant in protecting primary hepatocytes from oxidative damage induced by aflatoxin B1, a well recognized hepatocarcinogen.

Apoptosis is now recognized as an important mode of cell death in response to cytotoxic treatments⁷⁾. It has been well documented that the administration of many natural compounds with anti-tumor activities triggers the apoptotic death of cancer cells⁸⁻¹³⁾. The present study was designed to investigate whether the cytotoxic effects of EA were mediated via an apoptotic mechanism. In this study, we evaluated the growth-inhibitory effect of EA on a human uterine leiomyomal smooth muscle cells (ULSMC). The induction of apoptosis was examined by morphological changes, DNA fragmentation and cell cycle/DNA content analysis. Furthermore, the involvement of intracellular glutathione (GSH) and mitochondria in EA-induced apoptosis was also investigated.

Materials and Methods

1. Chemicals

Minimum essential medium (MEM) and fetal bovine serum (FBS) were obtained from Life Technologies (Faisley, Scotland). Propidium iodide (PI) was purchased from Molecular Probes (Eugene, OR). The TdT-mediated dUTP nick end labeling (TUNEL) assay kit was from Boehringer Mannheim (Germany). All chemicals used were from Sigma (St. Louis, MO).

2. Preparation of herbal extract

The plant was collected in Kyungju city, the Republic of Korea, and sample and voucher specimen are kept in the herbarium (number 4-99-221) of the College of Oriental Medicine, Dongguk University. The plant samples were extracted 3 times with water at boiling temperature for 5 h. The extracts were filtered through a 0.45 m filter and lyophilized. The w/w yield of extracts was about 2.25%. For the bioassay test, samples were dissolved in DMSO and further diluted in culture media.

3. Tissue collection for uterine leiomyomal smooth muscle cell (ULSMC)

Human ULSMC were used in this study. In brief, uterine leiomyoma and adjacent normal myometrial tissues were obtained from women with regular menstrual cycles who underwent abdominal hysterectomy for medically indicated reasons at Dongguk University Hospital. The use of uterine tissues for culture experiments was approved by the institutional review board. The age of the subjects is in the range of 30~43 years (mean age, 37 years) and none had received hormonal therapy for at least three cycles before surgery. Informed consent was obtained from each subject before surgery for the use of uterine tissues

for the present study. Each uterine specimen was examined by a pathologist for histological examination and dating of the endometrium.

4. Cell culture

Uterine leiomyoma tissues and adjacent normal myometrial tissues were dissected from endometrial cell layers, washed in phosphate buffered saline (PBS), cut into small pieces, and digested in 0.2% collagenase (wt/vol) at 37°C for 3~5 hours. The ULMC was collected by centrifugation at 460 g for 5 min and washed several times with DMEM containing 1% antibiotic solution. The isolated ULSCM was, respectively, plated in 75 cm² flasks at approximate density of 5~105 cells/flask and subcultured for 120 hours at 37°C in a humidified atmosphere of 5% CO₂-95% air in DMEM supplemented with 10% FBS (vol/vol). The trypan blue exclusion test was used to determine the cell viability. Characterization of the cultured cells was examined using the immunostaining with monoclonal antibodies to a muscle-specific protein desmin, to a class of intermediate filament protein present in fibroblast vimentin, and to a cytoskeletal protein for epithelial cells cytokeratin. Thereafter, the cultured cells were stepped down to serum-free conditions by incubating in serum-free DMEM. The cultured cells were at approximately 40~50% confluence, and monolayer cultures were maintained in serum-free DMEM for an additional 72 hours.

Each cell line was also cultured in a 5% CO₂ humidified incubator at 37°C. RPMI1640 (GIBCO BRL, Rockville, MD, USA) containing 10% FBS which was used as the growth medium for all the three types of cells.

5. Treatment with EA

Cells were cultured in complete DMEM or MEM (containing 10% FBS, 100 units/mL penicillin, 100 µg

/mL streptomycin (pH 7.4)) in 75 cm² tissue culture flasks at 37°C in 5% CO₂. Cells normally reached about 60% confluence at the time of treatment. Cells were treated with EA in FBS-free medium and incubated for designated periods of time.

6. Effect of EA on ULSCM growth

Cells were first cultured in 96-well microplate (1 × 10⁴ cells/well in 100 µl complete MEM) for 12 h, and then incubated with different concentrations of EA in serum-free medium. At the end of incubation, a tetrazolium dye colorimetric test (MTT test) was used to monitor cell growth, as indicated by the conversion of the tetrazolium salts to the colored product, formazan, the concentration of which can be measured spectrophotometrically¹⁴⁾.

7. Determination of cytotoxicity

Lactate dehydrogenase (LDH) activity was determined with an Abbott VP Biochemical Analyzer using commercial test kit (Abbott Laboratories, Chicago, IL)¹⁵⁾. The percentage of LDH leakage from cells was used as the index of cell viability, which was calculated according to the following formula: % LDH leakage = (LDH activity present in the medium after incubation / total LDH activity in cells) × 100.

8. Morphological study

Morphological changes of the cellular nuclear after treatment were studied using acridine orange/ethidium bromide staining¹⁶⁾. After harvesting by trypsinization, cells were washed with PBS once. Twenty-five micro litres of the cell suspension was then mixed with 1 µl of the dye mixture, containing 100 µg/mL acridine orange and 100 µg/mL ethidium bromide in PBS. After staining, cells were visualized immediately under a fluorescence microscope.

9. TUNEL assay

DNA fragmentation was determined by the TUNEL assay¹⁷. The experiment was conducted according to the protocol established in our laboratory¹⁸. Using flow cytometry, 10000 cells in each group were analyzed, and the data obtained were analyzed using WinMDI 2.7 software (Scripps Institute, La Jolla, CA).

10. Measurement of sub-G1 cells

EA-induced DNA fragmentation was also studied by sub-G1 cell analysis. It is well recognized that DNA fragmentation during apoptosis results in the appearance of cells with low DNA stainability, which is shown as a sub-G1 peak in cell cycle/DNA content analysis using PI staining¹⁹. Briefly, after the designated treatment, cells were washed, resuspended in PBS and then fixed with ice-cold 70% ethanol at 4 °C for 2 h. The fixed cells were incubated with freshly prepared PI-staining buffer (0.1% Triton X-100 in PBS, 20 µg/mL PI, 200 µg/mL RNase) for 30 min at room temperature. The cell cycle was analyzed using flow cytometry.

11. Determination of intracellular GSH content

The determination of intracellular GSH content was conducted according to the method of Hissin and Hilf²⁰, with modifications¹⁸. Briefly, after treatment, cell homogenates were prepared in 0.1 M sodium phosphate-5 mM EDTA buffer (pH 8.0), and then 0.25% HPO₃ was added to precipitate protein. After centrifugation (59000 × g for 5 min at 4 °C), the supernatant was used for GSH assays. The fluorescence intensity of o-phthalaldehyde (OPT) was monitored at 420 nm, with the excitation wavelength set at 350 nm. The GSH content in ULSCM was expressed as nmole /10⁶ cells.

12. Assessment of mitochondrial membrane potential by flow cytometry

The level of mitochondrial membrane potential was determined by flow cytometry after staining with Rh123, a cationic lipophilic fluorochrome with a distribution to the mitochondrial matrix which correlates with the mitochondrial membrane potential²¹. A stock solution of Rh123 was prepared at 1 mg/mL in distilled water and stored in the dark at 4 °C. It was added at the final concentration of 5 µg/mL in a 0.5 mL cell suspension adjusted at 106/mL in PBS. After incubation at 37 °C for 30 min, the cells were washed and resuspended in 0.5 mL PBS for flow cytometry assays, with the excitation wavelength at 488 nm and the emission wavelength at 525 nm.

13. Statistical analysis

All data are presented as mean ± standard deviation (SD) from at least two sets of independent experiments. The difference among different groups was analyzed using one-way analysis of variance (ANOVA) with Scheffe's test or the Student's *t*-test. AP value of less than 0.05 was considered statistically significant.

Results

1. Effect of EA on cell growth

Fig. 1 illustrates the effect of EA on ULSCM proliferation as measured by the MTT test. It was found that after incubation with cells for 24 h, EA caused a dose-dependent reduction in cell proliferation. At 200 µg/mL, cell growth of the EA-treated group was only 14.6% of the control. As shown in Fig. 1B, the growth-suppression effect was evident from 12 h onwards (*p*<0.05). These findings indicate that EA strongly inhibited the proliferation of ULSCM in a dose- and time-dependent manner.

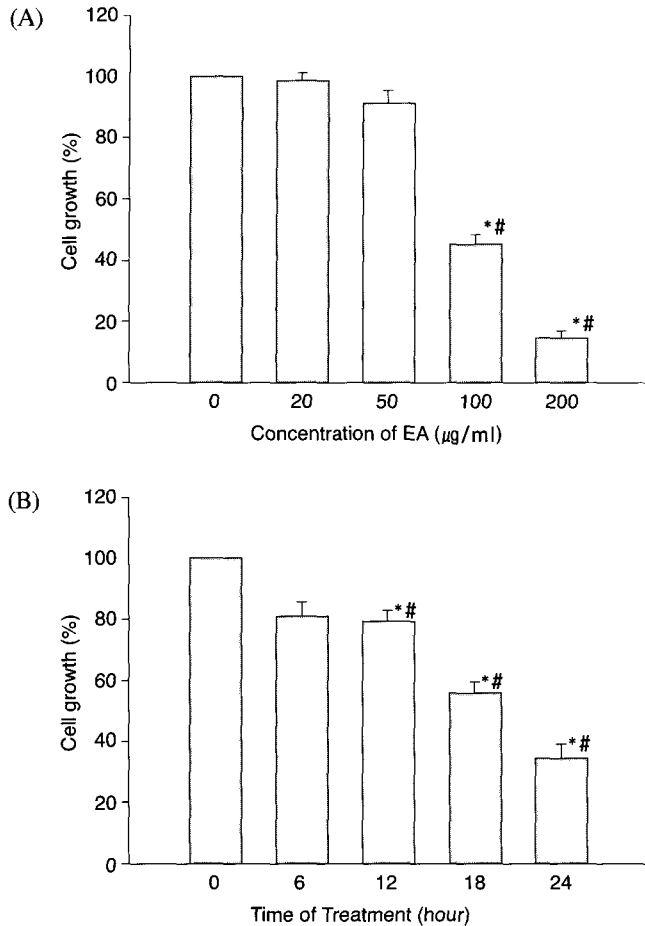


Fig. 1. The Effect of EA on cell growth in ULSMC measured by the MTT test.

ULSMC were incubated with EA: (A), 0-200 µg/mL for 24 h in the dose-response study; or (B), with 100 µg/mL in the time-course study. Data are presented as mean±SD (n=8). The percentage of cell growth in the control group was treated as 100%. **p*<0.05 compared with the control, and #*p*<0.05 compared with: (A), EA of 20 µg/mL; or (B), 6-h treatment (one-way ANOVA with Scheffe's test).

2. The cytotoxicity of EA on ULSMC

EA-induced cytotoxicity, measured as the percentage of LDH leakage, is shown in Fig. 2. After 24 h of incubation at the lowest EA concentration (20 µg/mL), no significant difference was found from that of the control. However, when EA concentration increased, a

dose-dependent response in LDH leakage in ULSMC was observed, which indicates the presence of cell injury caused by EA. In the time-course study, it was found that a significant increase of LDH activity in the medium was only observed when cells were treated with 100 µg/mL EA for more than 18 h.

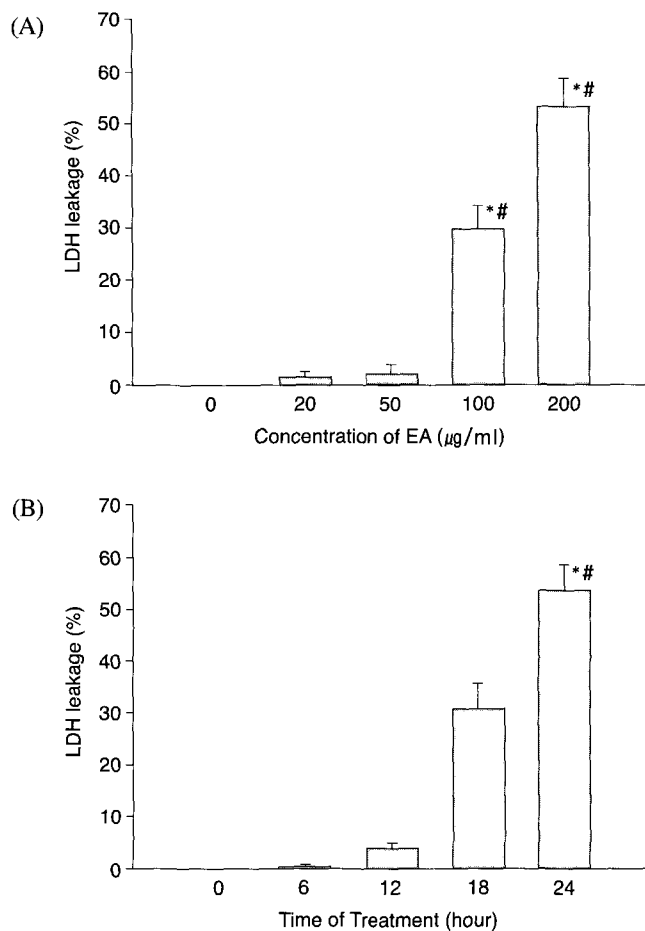


Fig. 2. EA-induced cytotoxic effects determined by LDH leakage in ULSMC.

ULSMC were cultured in 75 cm² culture flasks and incubated: (A), with EA (5-200 µg/mL) for 24 h in the dose-response study; or (B), with 100 µg/mL EA in the time-course study. Data are presented as mean ± SD (n=4). *p<0.05 compared with the control, and #p<0.05 compared with: (a), EA of 20 µg/mL; or (b), 6-h treatment (one-way ANOVA with Scheffe's test).

3. EA-induced apoptosis in ULSMC

In the present study, the cells were evaluated for evidence of apoptosis by three assays: (a), a morphological study using acridine orange/ethidium bromide staining; (b), the TUNEL assay; and (c), sub-G1 cell analysis.

Typical morphological changes induced by EA in ULSMC are demonstrated in Fig. 3. It was observed that EA treatment caused evident cytoplasmic and nuclear shrinkage, chromatin condensation and membrane blebbing, all characteristic morphological alterations of apoptosis²². These morphological changes were obvious as early as 3 h after incubation with EA



Fig. 3. Morphological changes in ULSMC.

Cells were stained with acridine orange/ethidium bromide and examined under a fluorescence microscope. A) control cells; B) cells treated with 200 $\mu\text{g}/\text{mL}$ EA; C) cells treated with 250 $\mu\text{g}/\text{mL}$ EA for 24 h. Clear cell shrinkage, membrane blebbing and chromatin condensation were observed in EA-treated cells.

and lasted throughout the whole period of treatment. After both control cells and cells treated with 200 $\mu\text{g}/\text{mL}$ EA for 24 h in the TUNEL assay, the percentage of apoptotic cells was calculated by the positive staining of nuclei with fluorescein, and the results are summarized in Fig. 4. It was found that EA-induced apoptosis was both time- and dose-dependent. No obvious changes were observed when cells were treated with 20 $\mu\text{g}/\text{mL}$ EA for 24 h. A substantial increase of apoptotic cells was observed from 50 $\mu\text{g}/\text{mL}$ onwards. About 55% of cells were apoptotic when treated with 200 $\mu\text{g}/\text{mL}$ EA for 24 h; this is consistent with the results of the LDH and MTT tests. In addition, the percentage of apoptotic cells found in the TUNEL assay increased markedly when cells were treated with EA for 6 h (Fig. 4), while no significant changes of LDH leakage were found (Fig. 2), suggesting that EA-induced DNA damage (strand breaks) preceded the disruption of cell membrane integrity.

EA-induced apoptosis in ULSMC was also evaluated by sub-G1 cell analysis with PI staining. The changes of cell cycle profile induced by EA (200 $\mu\text{g}/\text{mL} \times 24$ h) were examined. Cells incubated with EA resulted in the accumulation of a discrete sub-population of signals under the G1 cell cycle region. The increase of apoptotic sub-G1 cells was found to be time- and dose-dependent (Fig. 5). It is interesting to note that this response is in accordance with that of LDH leakage (Fig. 2), indicating that cell cycle change is a rather late event in apoptosis, compared with morphological alterations and the appearance of TUNEL-positive cells.

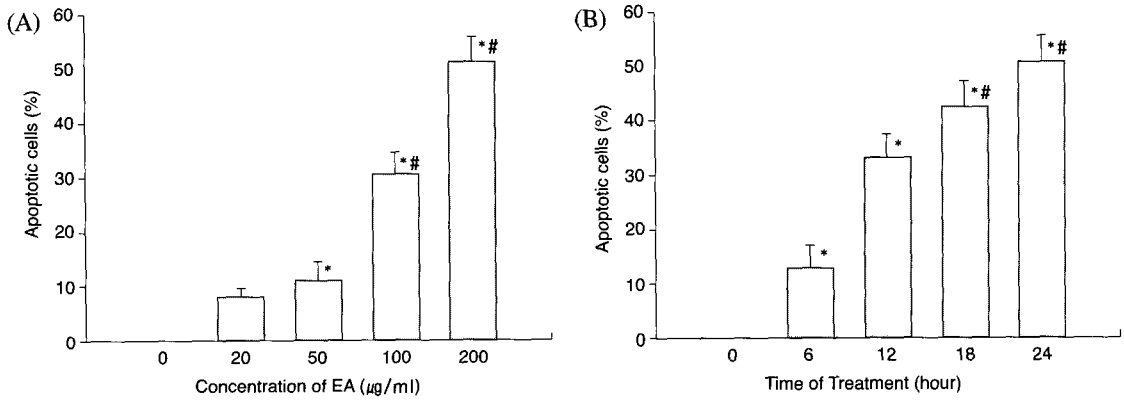


Fig. 4. EA-induced apoptosis in ULSMC determined by TUNEL assay: (A), dose response for 24 h; and (B), time-course study with 200 µg/mL EA.

The data were obtained using flow cytometry based on 10000 cells from each group, and are presented as mean ± SD of three independent experiments. * $p < 0.05$ compared with the control; and # $p < 0.05$ compared with (A), EA of 20 µg/mL; or (b), 6-h treatment (one-way ANOVA with Scheffe's test).

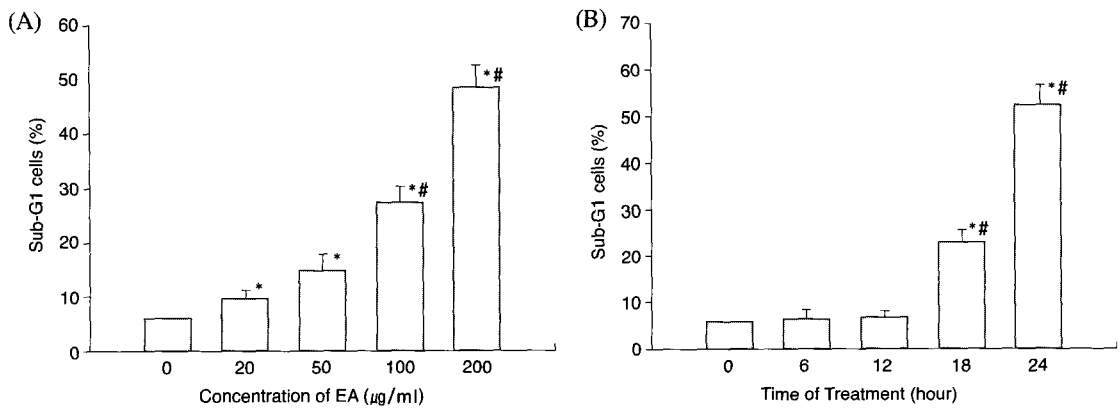


Fig. 5. EA-induced apoptosis in ULSMC determined by cell cycle/DNA content analyses: (A), dose response for 24 h; and (B), time-course study with 200 µg/mL EA.

The data were obtained using flow cytometry based on 10000 cells from each group, and are presented as mean ± SD of two independent experiments. * $p < 0.05$ compared with the control; and # $p < 0.05$ compared with (A), EA of 20 µg/mL; or (B), 6-h treatment (one-way ANOVA with Scheffe's test).

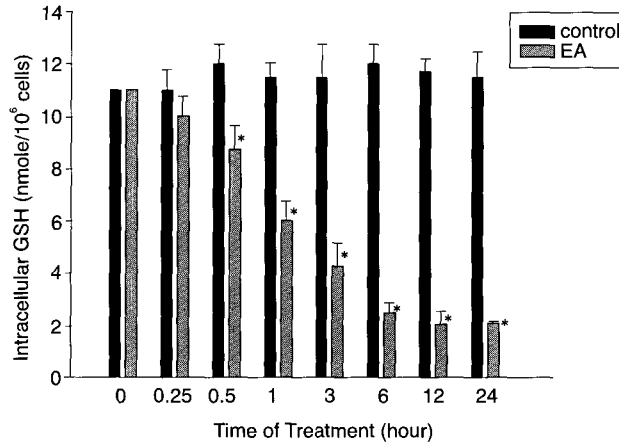


Fig. 6. Changes of intracellular GSH content induced by EA.

GSH content was measured by the OPT method at 15 and 30 min, and 1, 3, 6, 12 and 24 h after treatment with EA (200 $\mu\text{g}/\text{mL}$). Data are presented as mean \pm SD (n=3). * $p < 0.05$ compared with the control group (one-way ANOVA with Student's t-test).

4. Effect of EA on intracellular GSH content

Fig. 6 shows the result of the time-course study of intracellular GSH content in ULSMC for up to 24 h. As seen, there was a sharp decline in the level of GSH within the first hour of 200 $\mu\text{g}/\text{mL}$ EA treatment. The content of GSH progressively decreased with the time of incubation, but the change tended to be stable from 6 h onwards. At 24 h, the GSH concentration in EA-treated group was only 2.3 nmole/10⁶ cells, which was about five times lower than the control value (11.2 nmole/10⁶ cells). Meanwhile, GSH content in the control group remained at a relatively high level within the incubation period. This finding suggests that EA caused intracellular GSH depletion.

5. Effect of EA on mitochondria membrane potential

Fig. 7 shows the changes of mitochondrial membrane potential both in control and EA-treated ULSMC. Treatment with 200 $\mu\text{g}/\text{mL}$ EA results in a dramatic loss of mitochondrial membrane potential as evidenced by

the decline of Rh123 fluorescence intensity. In EA-treated cells, the mean fluorescence intensity began to decrease significantly as early as 15 min after EA exposure, and progressive reduction was observed from 15 min onwards. At 24 h, the control cells exposed to Rh123 exhibit bright green fluorescence with a mean fluorescence intensity of 12.5, which is slightly lower than the initial value ($p < 0.05$). In contrast, exposure to EA caused a predominant decline in Rh123 fluorescence, with the mean value being only four. These results clearly demonstrate a EA-dependent decrease in mitochondrial membrane potential. Furthermore, this event happened prior to the onset of morphological and biochemical features of EA-induced apoptosis.

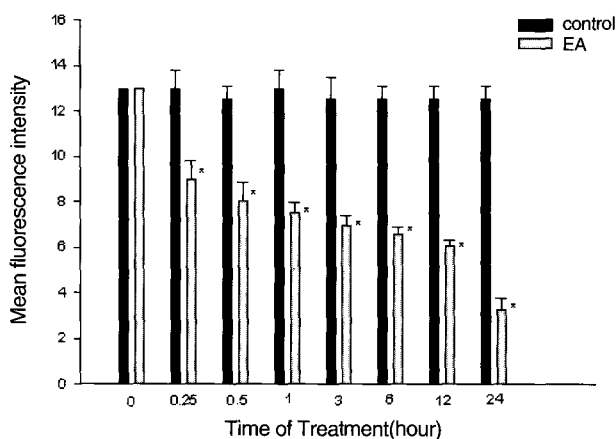


Fig. 7. EA-induced mitochondrial membrane potential alteration in ULSCM.

Time-dependent changes of mitochondrial membrane potential in ULSCM. Mitochondrial membrane potential was measured by flow cytometry with Rh123 at 15 and 30 min, and 1, 3, 6, 12 and 24 h after treatment with EA (200 $\mu\text{g}/\text{mL}$). Data are presented as mean \pm SD of two independent experiments. * $p < 0.05$ compared with the control group (one-way ANOVA with Student's *t*-test).

Discussion

As part of our ongoing study on the anti-tumor potential of EA, the main aim of the present investigation was to explore the effect of EA on cell growth and the induction of apoptosis in a human ULSCM line. The present study demonstrates that EA possesses growth-inhibitory capability against a human ULSCM (Fig. 1). This finding is in agreement with previous studies showing that EA inhibits the growth of cultured cell lines derived from human carcinomas⁴. Fig. 2 shows that EA at concentration of 50 $\mu\text{g}/\text{mL}$, and above, significantly affected the viability of ULSCM, suggesting that the observed growth inhibition was caused by a cytotoxic, rather than a cytostatic, effect of EA. We further investigated whether the cytotoxic effect was mediated via an apoptotic mechanism. As evidenced by morphological alterations (Fig. 3) and characteristic flow cytometric features in TUNEL and cell cycle analysis (Fig. 4 and Fig. 5), it appears that

apoptosis is the main mechanism for cell killing in the presence of EA.

EA has been reported to show cytotoxic effects in vitro on various tumor cells. Kim³⁾ and Cha³⁾ et al found that within a range of concentration between 5 and 100 $\mu\text{g}/\text{mL}$, methanol extracts of EA were able to inhibit the proliferation of cells derived from human carcinomas of the cervix (Hela cell) and larynx (Hep-2 cell). However, the mechanisms involved in these observations are largely unclear. Our study appears to be the first to demonstrate that the induction of apoptosis is the major pathway in EA-caused cell death. Due to the critical role of apoptosis in tissue homeostasis and cancer development, the modulation of apoptosis has become an interesting target in both therapeutic and preventive approaches in cancer²³. Although data from this study demonstrate that EA was able to inhibit the growth of cancer cells in vitro, the in vivo anti-tumor potential of EA remains to be determined. Nevertheless, EA, as a herbal medicine, has its unique properties, including:

(a), no known adverse effect; (b), no difficulty for oral consumption; (c), low cost; and (d), a long history of use by the human population²¹, all of which are indicative of its potential application as an anti-tumor agent.

The concentrations of organic extracts used in the earlier studies were usually within the range of 5-50 $\mu\text{g}/\text{mL}$, and when converted to the whole water extract it is quite comparable with the dosage used in the present study. It is important to note that when used at its equivalent dose in the crude extract, EA was not as effective as the whole extract in protecting primary hepatocytes from aflatoxin B1-induced cytotoxicity. The whole crude extract was thus used in the present study.

In order to elucidate the possible mechanism involved in the induction of apoptosis, the effects of EA on intracellular GSH content and mitochondrial membrane potential were also investigated. Our results indicate that depletion of GSH is an early event in EA-induced apoptotic process. It occurs before cells exhibit the morphological and biochemical changes of apoptosis. Several earlier studies have also demonstrated that the onset of apoptosis is associated with a fall of intracellular GSH in different cellular systems²⁴. The role of GSH in EA-induced apoptosis is considered of significant importance, based on two facts: (1), GSH is an important cellular thiol which is regarded as the major determinant of the intracellular redox potential, and on the other hand, apoptosis may be regulated by the redox status within the cell²⁵; and (2), the loss of GSH was shown to be tightly coupled with a number of down-stream events in apoptosis, including caspase activation and events in chromatin²⁶. The decrease of GSH induced by EA may be due to either increased degradation or decreased synthesis. It is unlikely to be caused by increased efflux of GSH, since the GSH concentration in the culture medium of EA-treated

group was not changed compared with that of the control throughout the whole incubation period. (data not shown)

Recent studies have shown that the nuclear features of apoptosis are preceded by alterations in mitochondria function and structure²⁷. Results from the present study clearly demonstrated that ULSCM treated with EA exhibited an early reduction of mitochondrial membrane potential and such changes occurred long before DNA fragmentation(Fig. 7), indicating the critical role of mitochondrial membrane potential in EA-induced apoptosis. Indeed, the role of mitochondria in the apoptotic process has been well documented. The disruption of mitochondrial membrane potential and subsequent nuclear apoptosis can not be dissociated²⁸. Possible mechanisms include the release of mitochondrial proapoptotic factors, such as cytochrome c²⁹, and the apoptosis-inducing factor³⁰. Whether such mechanisms also involved in EA-treated ULSCM remains to be further studied.

In summary, the present study demonstrates that EA has profound effects on ULSCM in vitro. It reduces the proliferation of these cells, causes changes in their morphology, and induces cell death by apoptosis. These responses are both time- and dose-dependent. It is believed that the depletion of intracellular GSH and reduction of mitochondrial membrane potential are involved in the induction of apoptosis by EA in ULSCM.

References

1. Kitanaka, S., Takido, M., Mizoue, K. and Nakaike, S. Cytotoxic cardenolides from woods of *Euonymus alata*. Tokyo. Chem. Pharm. Bull. 1996;44:615-617.
2. Change HM, Danshen PP. P. Pharmacology and applications of chinese materia. Medica World Scientific. Singapore. 1986:255-268.
3. Kim CH. Effect of buthanol and methanol extracts

- from *Euonymus Alatus* on matrix metalloproteinase-9 in cervical epithelial carcinoma cells. Korean Journal of OB. &GY. 2003;16(1):143-150.
4. Cha BY, Park CJ, Lee DG et al. Inhibitory effect of methanol extract from *Euonymus Alatus* on matrix metalloproteinase-9. J. Ethnopharmacol. 2002;85:163-167.
 5. Huang KC. The pharmacology of Chinese herbs. CRC Press, Boca Raton. 1993:93-94.
 6. Kitanaka S., Takido M., Mizoue K., Nakaike S. Cytotoxic cardenolides from woods of *Euonymus alata*. Chemical and pharmaceutical bulletin. Tokyo. 1996;44:615-617.
 7. Kerr JFR, Winterford CM, Harmon BV. Apoptosis its significance in cancer and cancer therapy. Cancer. 1994;73:2013-2026.
 8. Paschka AG, Butler R, Young CYF. Induction of apoptosis in prostate cancer cell lines by the green tea component, (-)-epigallocatechin-3-gallate. Cancer Lett. 1998;130:1-7.
 9. Yanagihara K, Ito A, Tuge T, Numoto M. Antiproliferative effects of isoflavines on human cancer cell lines established from the gastroin testinal tract. Cancer Res. 1993;53:5815-5821.
 10. Diomede L, Piovani B, Re F, Principe P, Colotta F, Modest EJ, Salmons M. The induction of apoptosis is a common feature of the cytotoxic action of ether-linked glycerophospholipids in human leukemic cells. Int. J. Cancer. 1994;57: 645-649.
 11. Jiang B, Li DD, Zhen YS. Induction of apoptosis by enediyne antitumor antibiotic C1027 in HL-60 promyelocytic leukemia cells. Biochem. Biophys. Res. Commun. 1995;208:23-244.
 12. Piazza GA, Kulchak Rahm AL, Krutsch M, Sperl G, Paranka NS, Gross PH, Brendel K, Burt RW, Alberts DS, Pamukcu R. Antineoplastic drugs sulindac sulfide and sulfone inhibit cell growth by inducing apoptosis. Cancer Res. 1995; 55:151-159.
 13. Smets LA. Programmed cell death (apoptosis) and response to anti-cancer drugs. Anti-Cancer Drugs. 1994;5:3-9.
 14. Hansen MB, Nielsen SE, Berg K. Re-examination and further development of a precise and rapid dye method for measuring cell growth/cell kill. J. Immunol. Methods. 1989;119:203-210.
 15. Shen HM, Ong CN, Shi CY. Involvement of reactive oxygen species in aflatoxin B1-induced cell injury in cultured rat hepatocytes. Toxicology. 1995;99:115-123.
 16. MacGahon AJ, Martin SJ, Bissonnette RP, Mahboubi A, Shi Y, Mogil RJ, Hishioka WK, Green DG. The end of the (cell) line: methods for the study of apoptosis in vitro. Methods Cell Biol. 1995;46:153-181.
 17. Gavrieli Y, Sherman Y, Ben-Sasson SA. Identification of programmed cell death in situ via specific labeling of nuclear DNA fragmentation. J. Cell Biol. 1992;119:493-501.
 18. Shen HM, Yang CF, Ong CN. Sodium selenite-induced oxidative stress and apoptosis in human hepatoma HepG2 cells. Int. J. Cancer. 1999;81: 820-82.
 19. Nicoletti L, Migliorati G, Pagliacci MC, Grignani F, Riccardi C. A rapid and simple method for measuring thymocyte apoptosis by propidium iodide staining and flow cytometry. J. Immunol. Methods. 1991;139:271-279.
 20. Hissin PJ, Hilf R. A fluorometric method for determination of oxidized and reduced glutathione in tissues. Ann. Biochem. 1976;74: 214-216.
 21. Sureda FX, Escubedo E, Gabriel C, Comas J, Camarasa J, Camins A. Mitochondrial membrane potential measurement in rat cerebellar neurons by flow cytometry. Cytometry. 1997;28: 74-80.
 22. Cohen JJ. Apoptosis. Immunol. Today 1993;14: 126-130.
 23. Ahmad N, Feyes DK, Nieminen AL, Agarwal R, Mukhtar H. Green tea constituent epigallocatechin-3-gallate and induction of apoptosis and cell cycle arrest in human carcinoma cells. J. Natl. Cancer Inst. 1997;89:1881-1886.
 24. Hall AG. The role of glutathione in the regulation of apoptosis. Eur. J. Clin. Invest. 1999;29:238-245.
 25. Watson RWG, Rotstein OD, Nathen AB. Thiolo-mediated redox regulation of neutrophil apoptosis. Surgery. 1996;120:150-158.
 26. Van den Dobbelaars DJ. Rapid and specific efflux of reduced glutathione during apoptosis induced by anti-

- Fas/APO-1 antibody. *J. Biol. Chem.* 1996;271:15420-15427.
27. Petit PX, Zamzami N, Vayssiere JL, Mignotte B, Kroemer G, Castedo M. Implication of mitochondria in apoptosis. *Mol. Cell. Biochem.* 1997;174:185-188.
 28. Kroemer G, Zamzami N, Susin S. Mitochondrial control of apoptosis. *Immunol. Today* 1997;18:44-5.1
 29. Kluck RM, Bossy-Wetzel E, Green DR, Newmeyer DD. The release of cytochrome c from mitochondria: a primary site for Bcl-2 regulation of apoptosis. *Science.* 1997;275:1132-1136.
 30. Susin SA, Zamzami N, Castedo M. Bcl-2 inhibits the mitochondrial release of an apoptogenic protease. *J. Exp. Med.* 1996;184: 1131-1141.